ON THE GROWTH AND ANNEALING OF STACKING FAULT TETRAHEDRA IN GOLD

by

K. C. Jain and R. W. Siegel

Department of Materials Science
State University of New York at Stony Brook
Stony Brook, L. I., New York

College of Engineering
Report #187
January, 1972

ON THE GROWTH AND ANNEALING OF STACKING FAULT TETRAHEDRA IN GOLD †

by

K. C. Jain and R. W. Siegel

Department of Materials Science
State University of New York at Stony Brook
Stony Brook, L. I., New York

ABSTRACT

The growth and annealing of stacking fault tetrahedra in quenched gold was studied by transmission electron microscopy using an interrupted anneal of matched bulk specimens. Specimens quenched from 930°C were initially aged to completely nucleate the tetrahedra. Subsequent measurements of the vacancy precipitate ensemble as a function of annealing time at 40°C showed continuous growth of the stacking fault tetrahedron distribution, while the tetrahedron density remained constant. The directly measured variation of precipitated vacancy concentration with time agreed reasonably well with that obtained under similar conditions from resistivity annealing studies. It is concluded that stacking fault tetrahedra exhibit continuous growth by the successive absorption of vacancies. Observations of the annealing of the final tetrahedron ensemble at temperatures up to 600°C showed shrinkage of the tetrahedra with no tendency for tetrahedron collapse. The results are discussed in terms of previous work.

---

† This work was supported by the National Science Foundation under Grants No. GK-3435 and No. GK-25134.

1. INTRODUCTION

Vacancy precipitation in quenched and aged gold leading to the formation of stacking fault tetrahedra has been widely investigated by transmission electron microscopy. It has been clearly demonstrated (see for example Meshii (1965)) that, under conditions suitable for tetrahedron formation, tetrahedron nucleation is completed in the early stages of aging. From this it could be logically assumed that stacking fault tetrahedra, once nucleated, grow in a well behaved manner presumably by a mechanism such as the vacancy supersaturation induced nucleation and migration of jog lines across the tetrahedron faces (de Jong and Koehler 1963, Kuhlmann-Wilsdorf 1965). However, the only published data on the direct observation of tetrahedron growth (Westdorp et al. 1964), while showing an increase in the average tetrahedron size with aging time, indicated considerably more complex behavior than would be expected from the normal growth of an ensemble of essentially randomly distributed vacancy precipitates (see fig. 4 of Westdorp et al. 1964). The present work was carried out, in part, in order to verify the generally accepted assumption that stacking fault tetrahedra do in fact grow in a simple, well behaved manner. Such normal tetrahedron growth has been an underlying assumption in recent investigations of the vacancy sink or climb efficiency of stacking fault tetrahedra in quenched gold (Siegel et al. 1968, Siegel et al. 1969, Jain and Siegel 1972). In addition, it was of interest to see whether the vacancy precipitation process could be followed with sufficient sensitivity and precision by electron microscopy to make feasible subsequent quantitative vacancy annealing studies using such a technique.

In addition to the investigations into the growth of stacking fault

tetrahedra, some interest has centered upon the mechanism of annealing of the stacking fault tetrahedra at high temperatures in gold. Two types of models for this process have been suggested: the continuous shrinkage of the tetrahedron by a jog-line or ledge climb mechanism similar to the growth model (Kuhlmann-Wilsdorf 1965, Jøssang and Hirth 1966), and the collapse of the metastable tetrahedron into a triangular Frank dislocation loop which subsequently shrinks by vacancy emission (Kuhlmann-Wilsdorf 1965, Escaig 1970). Experimental investigations supporting each of these models have been reported. The annealing of tetrahedra in bulk gold specimens by tetrahedron shrinkage has been observed by Segall et al. (1966) and was interpreted using a jog-line climb model. Nevertheless, Yokota and Washburn (1967) found that the dominant mechanism for tetrahedron annealing in thin gold foils was the collapse of the tetrahedra into stacking fault triangles on (111) planes followed by their shrinkage. However, the collapse of stacking fault tetrahedra into triangular dislocation loops is commonly observed, even at room temperature, in thin foils under the influence of thermally produced stresses in the electron microscope. This collapse is spatially random in nature, not all tetrahedra in a given area being affected, while larger tetrahedra tend to be more prone to collapse. Such observations were also made by Yokota and Washburn (1967) in their annealed foils. It was therefore of interest to further explore the mode of tetrahedron annealing representative of the bulk crystal.

In the present investigation, the isothermal growth at 40°C of a completely nucleated ensemble of stacking fault tetrahedra in gold was observed by transmission electron microscopy using an interrupted anneal of a set of matched samples from a given specimen. The directly measured precipitated

total vacancy concentration was then compared with existing electrical resistivity annealing data. Subsequent annealing at temperatures $\geq 525^{o}C$ of the resultant final tetrahedron ensemble in bulk samples was also observed.

2. EXPERIMENTAL PROCEDURE

Polycrystalline gold of 99.999 wt.% nominal purity (Cominco American, Inc.: Grade 59) was used for the experiment. The specimen was in the form of a ribbon with a cross-section 0.46 cm by 0.015 cm and with an approximately 8 cm long gauge length. The specimen shape and quenching technique used to obtain a matched set of samples with identical thermal histories were the same as those used in our previous experiments dealing with the growth of stacking fault tetrahedra in quenched gold (see for example Jain and Siegel (1972)). The specimen was annealed at $930^{o}C$ for 1 h by resistance heating and subsequently quenched from that temperature into distilled water at $25^{o}C$. The temperature of the specimen gauge length was maintained uniform to $\pm 3^{o}C$ at the quench temperature. The specimen then remained at $25^{o}C$ for 3 min before being placed in an oven at $(60 \pm 2)^{o}C$ for 10 min in order to completely nucleate the tetrahedra and initiate their growth in the specimen. The gauge length was then carefully cut, using a razor blade, into ten rectangular samples (0.23 cm by 1.6 cm); a process which took an additional 39 min at $25^{o}C$. In this manner, a set of matched samples containing essentially identical distributions of nucleated and partially grown tetrahedra was obtained.

After the cutting process was completed for all of the samples, one of them was stored at $-25^{o}C$ to be subsequently used for microscopic observation of the initial tetrahedron distribution and four others were placed in a temperature controlled aging bath at $(40.0 \pm 0.1)^{o}C$ for 0.5 h, 1.0 h, 2.0 h

and 4.0 h, respectively and then stored at -25^{o} to await observation in the electron microscope. The remainder of the samples were aged at 40^{o}C for 25 h in order that the vacancy precipitation or tetrahedron growth process could come to completion. Three of these fully aged samples were subsequently annealed in a furnace for 20 h at (525 ± 5)^{o}C, (600 ± 2)^{o}C and (700 ± 2)^{o}C, respectively and then furnace cooled.

Electron microscope samples were produced from the rectangular bulk samples by electropolishing using the standard KCN, etc. electrolyte (Thomas 1962). The samples used for determining the initial tetrahedron distribution and the subsequent isothermal growth data as a function of aging time were thinned by electropolishing at between -5^{o}C and 0^{o}C. The temperature of the electrolyte was controlled by a surrounding bath of acetone and ice and was constantly monitored by a thermometer. At no time during the preparation of these electron microscope samples were they subjected to temperatures higher than 21^{o}C, and this for only very short times required to transfer the samples from one bath to another and then to the electron microscope. The samples used for the observations of the tetrahedron distribution after completion of vacancy precipitation and those used to observe the effects of the high temperature bulk annealing were electropolished at 60^{o}C. Observation of the tetrahedron ensemble in each sample took place at room temperature immediately after thinning in a Philips EM 300 operated at 100 kV with a beam current of <30μA.

In order to specify the tetrahedron ensemble by its size distribution and density in each of the aged or annealed samples, three electron microscopy samples were prepared from each yielding about 30 to 40 micrographs. These micrographs were taken essentially at random throughout the thin foils

with the exclusion of regions in which perturbations to the precipitate structure had occurred due to the presence of other internal vacancy sinks (e.g., grain boundaries). In addition, selected area diffraction patterns were obtained in order to determine foil thicknesses using slip traces and twins in the usual manner. Almost all of the thin foil areas observed had a [001] normal orientation due to the strongly preferred orientation of the rolled specimen used. Therefore, apart from easy distinction between stacking fault tetrahedra and triangular Frank loops, it was obvious if a tetrahedron was intersected by the foil surface removing this possible ambiguity in the measurement of the true [110] edge lengths. The tetrahedron size distributions were obtained directly from contact prints of the electron micrographs, with a magnification of 62,000 X, using a Zeiss Particle Size Analyser. An average of 2400 ± 310 tetrahedra were measured in each of the six samples for the tetrahedron growth experiment, while an average of 1846 ± 3 were counted in the two tetrahedron annealing experiment samples.

3. RESULTS AND DISCUSSION

3.1. Stacking Fault Tetrahedron Growth

The results of the direct observations of the stacking fault tetrahedra in the six aged samples are presented in table 1 and fig. 1. In table 1 the tetrahedron density, N_s, and the root-mean-square edge length, L_{RMS}, of the tetrahedron distribution are shown for the various values of aging time, t_a, at 40°C after pre-aging for 10 min at 60°C and an additional 42 min at 25°C during specimen handling. Also tabulated is the fractional concentration of vacancies stored in the tetrahedra, $c_v^* = (a/4)\ N_s\ L_{RMS}^2$, where a is the lattice parameter. The mean deviations in these quentities from area to area within each sample are presented in all cases. Figure 1 shows the histograms

for the tetrahedron size distributions after each of the aging times, t_a. The N_s values in table 1 indicate that tetrahedron nucleation had been completed prior to the first observation, as had been planned, and that their density was constant (to within limits of ±5%) with an average value of $N_s = (2.0 \pm 0.3) \times 10^{15}$ cm^{-3}. Hence, the variation of tetrahedron size distribution with aging, shown in fig. 1, represents only the effects of tetrahedron growth. It can be seen that the observed growth was well behaved in detail, showing not only an increase in L_{RMS} with aging time, but also a continuous shift of the size distribution maximum to larger sizes and a broadening of the distribution with time. Such behavior was to have been expected for the normal continuous growth of an ensemble of randomly distributed precipitates.

These results may be contrasted with those of Westdorp et al. (1964) in which, while the average tetrahedron size increased with aging time, the size distribution contained two maxima at an early aging time. With subsequent aging the peak at larger tetrahedron sizes increased in magnitude, (but did not shift) while the peak at small edge length disappeared (see their fig. 4). In light of the results of the present investigation, these earlier observations must be considered spurious due to experimental difficulties. The conclusion that stacking fault tetrahedra, at least those with edge lengths $\gtrsim$ 100 Å, grow continuously as tetrahedra by the successive absorption of vacancies has been confirmed in detail by the present observations. It is likely that such tetrahedron growth takes place by the mechanism of jog line or ledge nucleation and subsequent migration across the tetrahedron faces (de Jong and Koehler 1963, Kuhlmann-Wilsdorf 1965).

In order to check the compatibility of these results from microscopic measurements with those obtained from macroscopic measurements which average

over far greater† specimen volume, a comparison was made between the directly determined fractional concentration of unprecipitated vacancies, $[c_v(t)/c_v(0)] = 1 - [c_v^*(t)/c_v^*(\infty)]$, as a function of aging time, shown in table 1, and that determined indirectly from electrical resistivity annealing. It should be pointed out that the above expression for $[c_v(t)/c_v(0)]$ assumes that all of the vacancies present at t = 0 (i.e., immediately after the quench) precipitate into observable clusters. This is a reasonable assumption for the present data since regions in which perturbing influences such as grain boundaries or other internal vacancy sinks were present were specifically excluded. In order to obtain $[c_v(t)/c_v(0)]$ from measurements of the specimen residual resistivity at 4.2°K, ρ, one can use the expression $[c_v(t)/c_v(0)] = [\rho(t) - \rho(\infty)]/[\rho(0) - \rho(\infty)]$, where the assumption that the contribution to the resistivity per precipitated vacancy is independent of cluster size is required. This latter assumption is not in general valid (see for example Siegel (1966)), but the above expression is sufficiently accurate for the present purposes of comparison.

The resistivity annealing at 40°C in a gold specimen quenched from 980°C measured by de Jong and Koehler (1963) was used for this comparison since it most closely resembled the present results in terms of both quenched-in vacancy concentration and annealing half-time, $t_{1/2}$, (i.e., the time at which $[c_v(t=t_{1/2})/c_v(0)] = 0.5$). These data are compared in fig. 2, in which $[c_v(t)/c_v(0)]$ is plotted as a function of the reduced annealing time, $t/t_{1/2}$. The annealing half-time at 40°C was estimated for the present experiment in the following manner. The total pre-aging time, t_o, prior to the first electron microscopy observations consisted of 10 min at 60°C plus 42 min at 25°C. These

---

† For example, the ratio of specimen volume sampled by an electrical resistivity measurement on a specimen of the dimensions used in this investigation to that actually sampled by electron microscopy would be $\sim 10^9$.

times were adjusted to 40°C using a Boltzmann factor normalization with an effective activation energy of 0.62 eV (Ytterhus and Balluffi 1965), yielding $t_o(40^oC) \simeq 53$ min. The effective aging times at 40°C were then given by $t = t_o + t_a$ and $t_{1/2}$ was readily determined. The values for $[c_v(t)/c_v(0)]$ and $t/t_{1/2}$ for the microscopy data are also presented in table 1.

A comparison the vacancy defect annealing data from electron microscopy and resistivity measurements in fig. 2 indicates reasonably good agreement between the two, especially in light of the only approximate equivalence of the detailed physical nature (i.e., $c_v(0)$, N_s, etc.) of the two systems from which the data were obtained. It is apparent that electron microscopy data, such as that of the present work, can be used to investigate quantitatively the vacancy precipitation process. For example, the direct observation of the growth of a given ensemble of vacancy precipitates at various aging temperatures would yield determinations of the effective activation energy for the vacancy precipitation process which were unaffected by such potential problems (Balluffi and Siegel 1965) as (1) annealing transients caused by rapid changes of aging temperature in slope change or related measurements, or (2) variability in vacancy sink structure from one quenched specimen to another in standard Arrhenius type measurements. Such a quantitative investigation is currently in progress by the authors.

3.2. Stacking Fault Tetrahedron Annealing

The observed changes in the fully aged tetrahedron size distribution and density resulting from annealing for 20 h at 525°C, 600°C and 700°C are presented in table 2 and fig. 3. Annealing was carried out on bulk samples, which were subsequently thinned for the electron microscopic observations of the tetrahedron ensembles. The tetrahedron density, N_s, root-mean-square edge

length, L_{RMS}, and atomic fraction of vacancies stored in the tetrahedra, c_v^*, are tabulated in table 2 along with the observed percentage losses in N_s and c_v^*. A comparison of the size distributions of fig. 3 clearly shows that shrinkage of the tetrahedron ensemble has taken place during the annealing at 525°C and 600°C. In addition, the micrographs analyzed for these samples showed no additional collapse of tetrahedra to stacking fault triangles as compared with the initial distribution. The observed reductions in L_{RMS} and N_s may thus be explained by assuming that either: (1) tetrahedron annealing occurred by the successive emission of vacancies by a ledge climb mechanism alone, or (2) in addition to tetrahedron shrinkage, some tetrahedra may have collapsed to Frank loops which subsequently annealed by vacancy emission and disappeared during the 20 h annealing periods.

Let us consider each of these possibilities in turn. Tetrahedron annealing via a ledge climb mechanism would be consistent with the theoretical predictions of Jøssang and Hirth (1966), based upon calculations of the relative energies of stacking fault tetrahedra and Frank loops in gold, and consistent with the conclusions of Segall et al. (1966) based upon their observations of tetrahedron annealing in bulk samples. There are, however, some minor discrepancies between the results of this latter work and those of the present investigation. Segall et al. (1966) observed that the size distribution maximum shifted to larger edge lengths after high temperature ($\geq$ 693°C) annealing (see their fig. 1) and suggested that this apparently spurious result probably resulted from excess vacancies being annihilated at the tetrahedra due to their rapid specimen cooling from these annealing temperatures. In the present investigation no such effect would have arisen since the samples were cooled slowly in the furnace and the equilibrium vacancy concentrations at 525°C and 600°C (Balluffi

et al. 1970) are $\lesssim$ 4% of the measured changes in c_v^* resulting from annealing. A decrease in L_{RMS} with a concomitant shift of the size distribution maximum to smaller edge lengths with annealing is to be expected, assuming that tetrahedron coarsening does not occur: an effect which has been neither observed by the present authors nor reported elsewhere. The specific annealing model used by Segall et al. (1966) to interpret their data predicts tetrahedron losses after annealing for 20 h at 525°C and 600°C of $\geq$ 66% and $\geq$ 97%, respectively as compared with the respective losses of only 8% and 26% observed in the present work. This discrepancy appears to contradict their specific model for tetrahedron annealing, but by so doing does not impugn a ledge climb annealing model in general.

An interpretation of the present results based upon a combination of tetrahedron shrinkage and collapse is somewhat more complex. The observation that considerable tetrahedron shrinkage has definitely taken place may lead one to a conclusion that tetrahedron collapse is not the predominant mechanism of tetrahedron annealing in constrast with the conclusion of Yokota and Washburn (1967). However, the situation is clouded by the possibility of impurity pinning effects (Escaig 1970). With reference to experimental observations of tetrahedron collapse and dislocation loop climb in gold (Yokota and Washburn 1966, Washburn and Yokota 1969), Escaig has developed a theoretical model for tetrahedron annealing from which it is concluded that tetrahedra with $L \gtrsim 230\text{Å}$ in pure gold should anneal by collapse to a Frank loop which shrinks by vacancy emission as soon as self-diffusion becomes possible. He further concludes that any greater tetrahedron stability is a result of impurity pinning of the dislocations involved. Based upon this model, the present results would have to be interpreted largely in terms of at least two impurity

pinning effects at the tetrahedra. On the one hand, some impurities would be required to stabilize the tetrahedra against collapse at the annealing temperatures while other impurities would be required to retard (but not prohibit) dislocation climb at the tetrahedra to account for the observed shrinkage. Tetrahedra which did break away from the pinning impurities could collapse to Frank loops which would presumably anneal rapidly at these temperatures (Washburn and Yokota 1969) assuming, of course, that they were not retarded by other impurities.

While this complex set of circumstances cannot be rejected out of hand, it would seem more reasonable to explain the present results solely in terms of tetrahedron annealing via a ledge climb mechanism, and to ascribe tetrahedron collapse to a primarily stress induced phenomenon which is especially parasitic in thin electron microscopy sample foils. It could then be concluded that the predominance of tetrahedron collapse found in annealed thin foils by Yokota and Washburn (1967) was largely an artifact of the thin foil experimental technique used. Such a conclusion would be consistent with the observed tetrahedron shrinkage found in both the present investigation and that performed by Segall et al. (1966) in which annealing of bulk samples was carried out, with thin foils only subsequently being made. Furthermore, the observation that significant tetrahedron annealing occurs only at temperatures $\gtrsim$ 600°C in bulk gold found by de Jong and Koehler (1963), Meshii (1965), Segall et al. (1966) and the present authors, in a variety of specimen materials of $\sim$ 99.999% nominal purity, is consistent with inherent tetrahedron stability greater than that proposed by Escaig (1970).

REFERENCES

Balluffi, R. W. and Siegel, R. W., 1965, Lattice Defects in Quenched Metals, edited by R. M. J. Cotterill et al., Academic Press, New York, 693.

Balluffi, R. W., Lie, K. H., Seidman, D. N. and Siegel, R. W., 1970, Vacancies and Interstitials in Metals, edited by A. Seeger et al., North-Holland Press, Amsterdam, 125.

de Jong, M. and Koehler, J. S., 1963, Phys. Rev. 129, 49.

Escaig, B., 1970, Cryst. Latt. Defects 1, 211.

Jain, K. C. and Siegel, R. W., 1972, Phil. Mag. 25, 105.

Jøssang, T. and Hirth, J. P., 1966, Phil. Mag. 13, 657.

Kuhlmann-Wilsdorf, D., 1965, Acta Met. 13, 257.

Meshii, M., 1965, Lattice Defects in Quenched Metals, edited by R. M. J. Cotterill et al., Academic Press, New York, 77.

Segall, R. L., Clarebrough, L. M. and Loretto, M. H., 1966, Phil. Mag. 14, 53.

Siegel, R. W., 1966, Phil. Mag. 13, 359.

Siegel, R. W., Balluffi, R. W. and Thomas, L. E., 1968, Acta Met. 16, 7.

Siegel, R. W., Jain, K. C., Schober, T., Balluffi, R. W. and Thomas, L. E., 1969, Cryst. Latt. Defects 1, 31.

Thomas, G., 1962, Transmission Electron Microscopy of Metals, John Wiley and Sons, New York, 162.

Washburn, J. and Yokota, M. J., 1969, Cryst. Latt. Defects 1, 23.

Westdorp, W., Kimura, H. and Maddin, R., 1964, Acta Met. 12, 495.

Yokota, M. J. and Washburn, J., 1967, Phil. Mag. 16, 459.

Ytterhus, J. A. and Balluffi, R. W., 1965, Phil. Mag. 11, 707.

Table 1. Data for the growth of stacking fault tetrahedra at 40°C in gold quenched from 930°C and initially aged for 10 min at 60°C plus 42 min at 25°C.

t_a(40°C) (h)	N_s (x 10^{15} cm^{-3})	L_{RMS} (Å)	c_v^* (x 10^{-4})	$c_v(t)/c_v(0)$	$t/t_{\frac{1}{2}}$
0	1.9 ± 0.4	246 ± 35	1.2 ± 0.2	0.66 ± 0.08	0.56
0.5	2.0 ± 0.3	280 ± 37	1.6 ± 0.3	0.54 ± 0.10	0.88
1.0	1.9 ± 0.3	310 ± 39	1.9 ± 0.2	0.46 ± 0.08	1.20
2.0	2.1 ± 0.3	344 ± 42	2.4 ± 0.2	0.30 ± 0.10	1.84
4.0	2.0 ± 0.4	375 ± 44	2.7 ± 0.2	0.21 ± 0.11	3.12
∞	2.0 ± 0.4	411 ± 62	3.4 ± 0.4	0	∞

Table 2. Data for the annealing of stacking fault tetrahedra in bulk gold samples held at various temperatures, T_A, for 20 hr.

T_A(20 h) (^oC)	N_s (x 10^{15} cm^{-3})	L_{RMS} (Å)	c_v^* (x 10^{-4})	$\Delta c_v^*/c_v^*(0)$ (%)	$\Delta N_s/N_s(0)$ (%)
initial distribution	2.0 ± 0.4	411 ± 62	3.4 ± 0.4	0	0
525 ± 5	1.8 ± 0.3	372 ± 38	2.5 ± 0.3	-27	-8
600 ± 2	1.5 ± 0.3	321 ± 31	1.5 ± 0.1	-57	-26
700 ± 2	nil	---	nil	-100	-100

FIGURE CAPTIONS

Fig. 1. Tetrahedron growth: variation of the tetrahedron size distribution with aging time, t_a, at 40°C after an initial pre-aging treatment of 10 min at 60°C plus 42 min at 25°C. During the pre-aging period nucleation was completed yielding a tetrahedron density of $N_s = (2.0 \pm 0.3) \times 10^{15}$ cm^{-3}. The histogram interval is $\Delta L = 30$ Å.

Fig. 2. A comparison of the fractional unprecipitated vacancy concentration, $c_v(t)/c_v(0)$, as a function of reduced annealing time, $t/t_{\frac{1}{2}}$, as obtained from resistivity annealing (de Jong and Koehler 1963) and measured directly by transmission electron microscopy.

Fig. 3. Tetrahedron annealing: changes in the tetrahedron size distribution resulting from annealing for 20 h at the temperatures, T_A, indicated. The histograms are normalized with respect to the initial distribution to show the observed tetrahedron losses. The histogram interval is $\Delta L = 30$ Å.

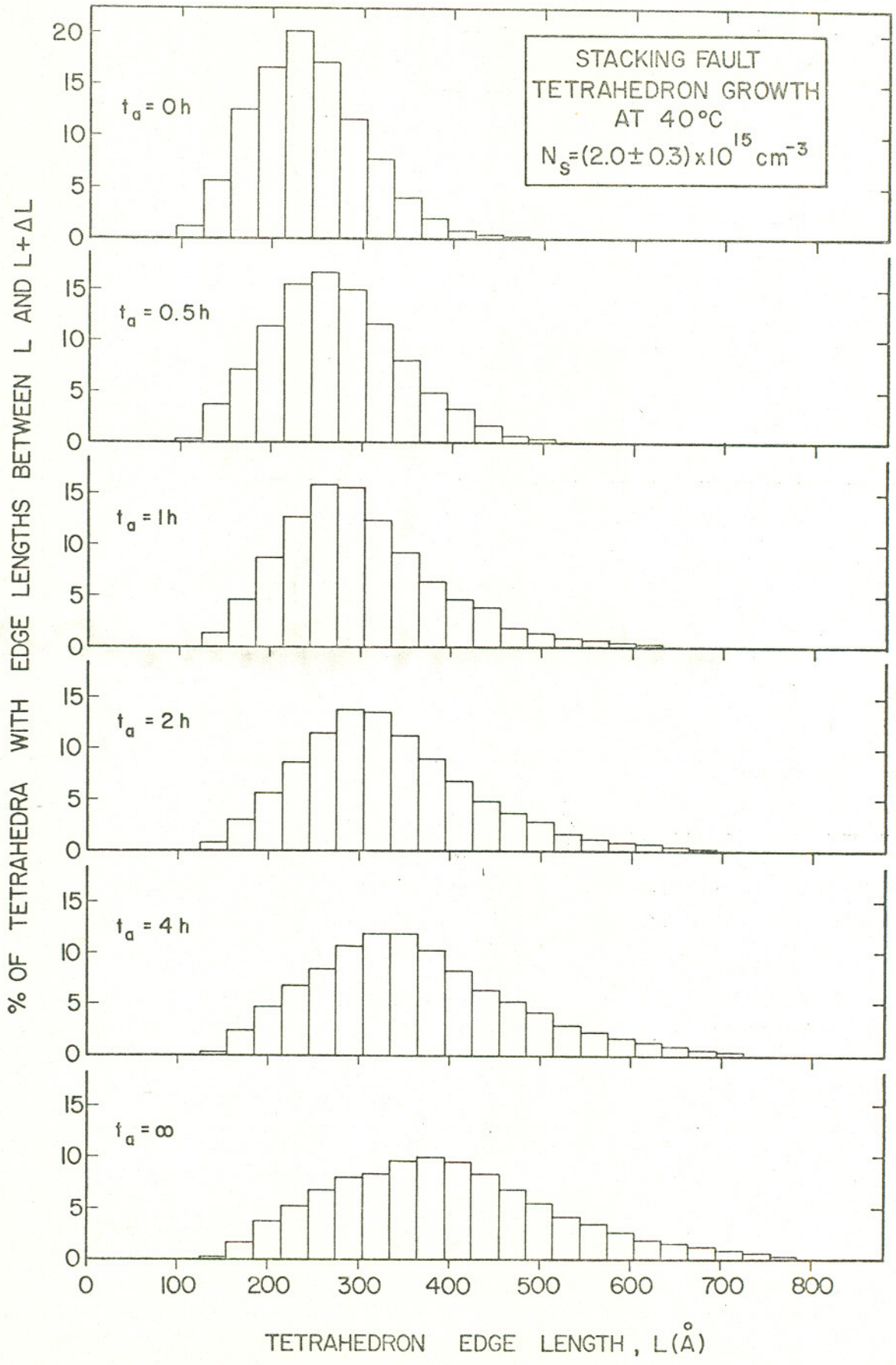
STACKING FAULT
TETRAHEDRON GROWTH
AT 40°C
$N_s=(2.0\pm0.3)\times10^{15}$ cm^{-3}
t_a = 0 h
t_a = 0.5 h
t_a = 1 h
t_a = 2 h
t_a = 4 h
t_a = ∞
% OF TETRAHEDRA WITH EDGE LENGTHS BETWEEN L AND L+ΔL
TETRAHEDRON EDGE LENGTH, L(Å)
0
100
200
300
400
500
600
700
800
5
10
15
20

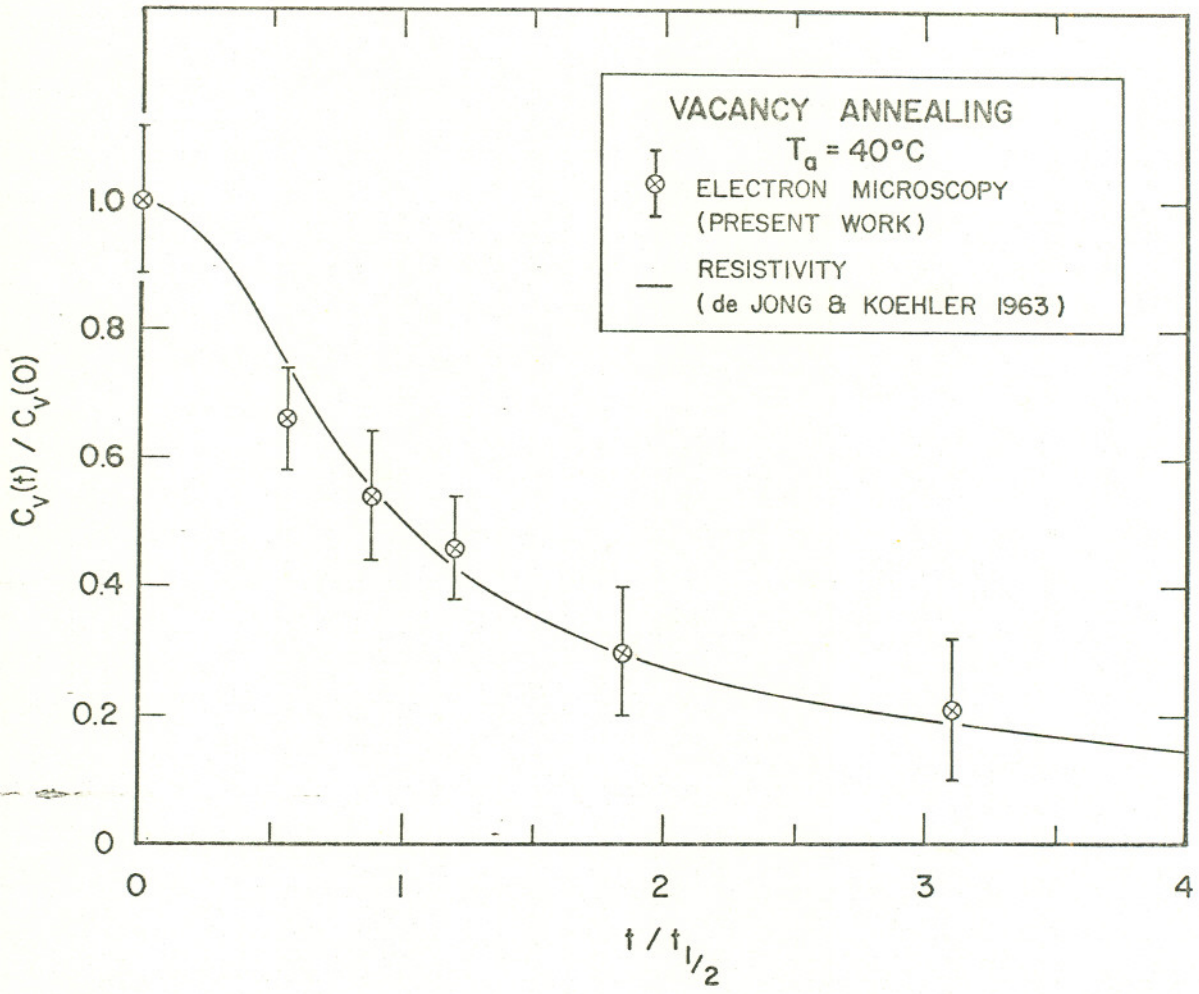
VACANCY ANNEALING
T_a = 40°C
ELECTRON MICROSCOPY
(PRESENT WORK)
RESISTIVITY
(de JONG & KOEHLER 1963)
$C_v(t) / C_v(0)$
1.0
0.8
0.6
0.4
0.2
0
0
1
2
3
4
$t / t_{1/2}$

% OF INITIAL TETRAHEDRA WITH EDGE LENGTHS BETWEEN L AND L + ΔL
TETRAHEDRON EDGE LENGTH , L (Å)
0
100
200
300
400
500
600
700
800
0
5
10
15
INITIAL DISTRIBUTION
T_A = 525°C
T_A = 600°C
STACKING FAULT TETRAHEDRON ANNEALING
t_A = 20h